J Physiol 597.12 (2019) pp 3217–3232

The Journal of Physiology

Alpha-melanocyte stimulating hormone increases the activity of melanocortin-3 receptor-expressing neurons in the ventral tegmental area

Katherine Stuhrman West[1,2], Chunxia Lu[3], David P. Olson[3] and Aaron G. Roseberry[1,2]

[1] *Department of Biology*
[2] *Neuroscience Institute, Georgia State University, Atlanta, GA, USA*
[3] *Department of Pediatrics, University of Michigan, Ann Arbor, MI, USA*

Edited by: David Wyllie & Diego Contreras

Key points

- Alpha-melanocyte stimulating hormone (α-MSH) is an anorexigenic peptide. Injection of the α-MSH analog MTII into the ventral tegmental area (VTA) decreases food and sucrose intake and food reward.
- Melanocortin-3 receptors (MC3R) are highly expressed in the VTA, suggesting that the effects of intra-VTA α-MSH may be mediated by α-MSH changing the activity of MC3R-expressing VTA neurons.
- α-MSH increased the firing rate of MC3R VTA neurons in acute brain slices from mice, although it did not affect the firing rate of non-MC3R VTA neurons.
- The α-MSH induced increase in MC3R neuron firing rate is probably activity-dependent, and was independent of fast synaptic transmission and intracellular Ca^{2+} levels.
- These results help us to better understand how α-MSH acts in the VTA to affect feeding and other dopamine-dependent behaviours.

Abstract The mesocorticolimbic dopamine system, the brain's reward system, regulates multiple behaviours, including food intake and food reward. There is substantial evidence that the melanocortin system of the hypothalamus, an important neural circuit controlling feeding and body weight, interacts with the mesocorticolimbic dopamine system to affect feeding, food reward and body weight. For example, melanocortin-3 receptors (MC3Rs) are expressed in the ventral tegmental area (VTA) and our laboratory previously showed that intra-VTA injection of the MC3R agonist, MTII, decreases home-cage food intake and operant responding for sucrose pellets. However, the cellular mechanisms underlying the effects of intra-VTA alpha-melanocyte stimulating hormone (α-MSH) on feeding and food reward are unknown. To determine how α-MSH acts in the VTA to affect feeding, we performed electrophysiological recordings in acute

Katherine West earned her doctorate degree in Neuroscience from Georgia State University (GSU) in 2018. During her time at GSU, she worked in Dr Aaron Roseberry's laboratory and studied how the mesocorticolimbic dopamine system regulates feeding, food reward and body weight, as well as how homeostatic feeding circuits interact with reward circuits. Her dissertation research focused on understanding how hypothalamic neuropeptides, such as α-melanocyte stimulating hormone, alter the activity of ventral tegmental area dopamine neurons. Dr West also has a bachelor's degree in Biology from GSU. She is currently an Instructor of Biology at Georgia Highlands College.

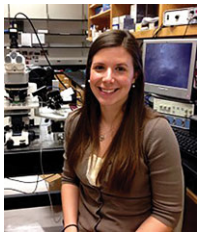

DOI: 10.1113/JP277193

brain slices from mice expressing enhanced yellow fluorescent protein in MC3R neurons to test how α-MSH affects the activity of VTA MC3R neurons. α-MSH significantly increased the firing rate of VTA MC3R neurons without altering the activity of non-MC3R expressing VTA neurons. In addition, the α-MSH-induced increase in MC3R neuron activity was independent of fast synaptic transmission and intracellular Ca^{2+} levels. Finally, we show that the effect of α-MSH on MC3R neuron firing rate is probably activity-dependent. Overall, these studies provide an important advancement in the understanding of how α-MSH acts in the VTA to affect feeding and food reward.

(Received 20 September 2018; accepted after revision 19 April 2019; first published online 13 May 2019)
Corresponding author A. G. Roseberry: Department of Biology, Georgia State University, PO Box 4010, Atlanta, GA 30302-4010, USA. Email: aroseberry@gsu.edu

Introduction

The World Health Organization estimates that obesity rates have almost tripled worldwide from 1975 onward (World Health Organization, 2018). The rapid rise in obesity is a major health concern because obesity increases the risk for many diseases, such as heart disease, diabetes, cancer and stroke (Afshin *et al.* 2017). The increased prevalence of obesity is largely attributed to an increase in food consumption (Finkelstein *et al.* 2005; Hall *et al.* 2009; Swinburn *et al.* 2009; Swinburn *et al.* 2011). Thus, an understanding of the mechanisms of food intake and weight gain is important for the development of new effective treatments that aim to prevent and reverse obesity.

The melanocortin system has been widely shown to play an important role in the control of feeding and body weight. This system encompasses two neuronal populations in the arcuate nucleus of the hypothalamus: pro-opiomelanocortin (POMC) expressing neurons and agouti-related protein/neuropeptide-Y (AgRP/NPY) expressing neurons, as well as the peptides released by these neurons and the downstream receptors of these peptides (Roseberry *et al.* 2015). POMC is a propeptide that is post-translationally processed to produce the melanocyte-stimulating hormones (α-, β-, and γ-MSH). α-, β-, and γ-MSH are agonists to the centrally expressed melanocortin receptors, melanocortin-3 and melanocortin-4 receptors (MC3/4Rs), whereas AgRP is an inverse-agonist to the MC3/4Rs (Roseberry *et al.* 2015). AgRP/NPY and POMC neurons respond to the energy state of an animal and function in an opposing manner. For example, an energy deficit or hunger state activates AgRP/NPY neurons (Hahn *et al.* 1998; Takahashi & Cone, 2005), whereas an energy surplus or satiated state activates POMC neurons (Singru *et al.* 2007; Wu *et al.* 2014). In addition, activation of AgRP/NPY neurons or injection of MC3/4R antagonists increases feeding (Fan *et al.* 1997; Ollmann *et al.* 1997; Aponte *et al.* 2011; Krashes *et al.* 2011), whereas activation of POMC neurons or injection of MC3/4R agonists decrease feeding (Fan *et al.* 1997; Pierroz *et al.* 2002; Aponte *et al.* 2011; Zhan *et al.* 2013). The melanocortin system is clearly an important regulator of food intake and substantial evidence indicates that this system interacts with other brain nuclei and neural systems, including the mesocorticolimbic dopamine system, to regulate food intake and body weight.

The mesocorticolimbic dopamine system is the primary neural circuit for reward and motivated behaviour and also regulates food reward, feeding and body weight (Wise, 2004; Lutter & Nestler, 2009; Kenny, 2011; Volkow *et al.* 2011; Roseberry *et al.* 2015). The mesocorticolimbic dopamine system comprises dopamine neurons in the ventral tegmental area (VTA) and the downstream targets of dopamine neurons such as the nucleus accumbens (NAc), prefrontal cortex (PFC), olfactory tubercle and hippocampus. Numerous studies show the importance of dopamine for food intake and food reward. For example, dopamine-deficient mice are aphagic (Zhou & Palmiter, 1995) and blocking dopamine receptors systemically or in the NAc decreases operant responding for food in rats (Beninger *et al.* 1987; Cousins *et al.* 1994; Koch *et al.* 2000). There is also substantial evidence that intra-VTA injection of a number of feeding-related peptides alters food intake and food reward (Liu & Borgland, 2015). This includes the injection of analogues of α-MSH and AgRP into the VTA. For example, our laborarory has shown that injection of the MC3/4R agonist, MTII, directly into the VTA decreases home-cage food intake, the intake of sucrose and saccharin intake in two-bottle choice tests, as well as operant responding for sucrose pellets, whereas injection of the MC3/4R antagonist, SHU9119, into the VTA increases home-cage food intake and operant responding for sucrose pellets (Roseberry, 2013; Yen & Roseberry, 2015; Shanmugarajah *et al.* 2017). Nevertheless, how α-MSH acts in the VTA at the cellular level to regulate feeding and other reward related behaviours is unknown.

Intra-VTA α-MSH may affect food intake and food reward by regulating VTA dopamine neuron activity. This is supported by studies first conducted in the 1980s

showing that intra-VTA injection of α-MSH increases dopamine turnover in the NAc (Torre & Celis, 1986, 1988). Furthermore, intra-VTA α-MSH and MC3/4R agonists increase dopamine-dependent behaviours, such as rearing, grooming and locomotor activity (Torre & Celis, 1986, 1988; Klusa *et al.* 1999; Sanchez *et al.* 2001). Additional evidence indicates that the melanocortin and mesocorticolimbic dopamine systems interact. POMC and AgRP neurons project to the VTA (King & Hentges, 2011; Dietrich *et al.* 2012) and both MC3Rs and MC4Rs are expressed in dopamine and non-dopamine VTA neurons (Roselli-Rehfuss *et al.* 1993; Liu *et al.* 2003; Lippert *et al.* 2014). However, the MC3R is expressed at much higher levels in the VTA than the MC4R (Roselli-Rehfuss *et al.* 1993; Liu *et al.* 2003; Lippert *et al.* 2014), suggesting that the effects of α-MSH and AgRP in the VTA are probably a result of the actions on MC3Rs. Thus, α-MSH can clearly act in the VTA to affect food intake, food reward and other reward behaviours, probably via activation of dopamine neurons expressing the MC3R. However, how α-MSH acts on MC3R-expressing VTA dopamine neurons to regulate food intake and reward behaviour and also to increase dopamine turnover in the NAc remains unknown. Thus, in the present study, we investigated whether α-MSH alters the activity of VTA MC3R expressing neurons using electrophysiology in brain slices from transgenic mice expressing enhanced yellow fluorescent protein (EYFP) in their MC3R neurons.

Methods

Ethical approval

All of the protocols and procedures were approved by the Institutional Animal Care and Use Committee at Georgia State University (approval reference no. A17016) and conformed to the NIH Guide for the Care and Use of Laboratory Animals. The investigators understand and complied with the ethical standards of the *Journal of Physiology* outlined in Grundy 2015 for all experiments (Grundy, 2015).

Animals

Male and female transgenic mice expressing EYFP in MC3R neurons (5–14 weeks old, 20–25 g, fed *ad libitum*) on a mixed C57/129 background were used in all experiments. Mice were generated by crossing transgenic mice expressing Cre recombinase tethered to the MC3R gene product by a 2A-self-cleaving peptide (Pei *et al.* 2018) (generously provided by Dr David P. Olson, University of Michigan, Ann Arbor, MI, USA) with a Cre inducible EYFP Ai3 transgenic mouse line from The Jackson Laboratory (Bar Harbor, ME, USA) (Stock # 007903). The specificity of Cre expression in MC3R neurons was confirmed previously in a separate study describing the creation and validation of this mouse (Pei *et al.* 2018). In total, 84 neurons from 60 mice were used in the experiments described in the present study. Five neurons from four mice were excluded from the study because the identity of the neuron was unconfirmed or the neuron died during the experiment.

RNAscope *in situ* hybridization (ISH) assay

RNAscope ISH was performed as described previously (Pei *et al.* 2018). Briefly, adult mice were quickly decapitated under anaesthesia. The brains were then removed, flash frozen with 2-methylbutane at –20°C and stored at –80°C. Coronal brain sections (16 μm) were cut with a cryostat and thaw mounted onto SuperFrost Plus Slides (Thermo Fisher Scientific, Waltham, MA, USA). ISH was performed according to the RNAscope® 2.5 HD Duplex Detection Kit User Manual for Fresh Frozen Tissue (Advanced Cell Diagnostics, Inc., Newark, CA, USA). The probes used were: RNAscope® Probe-Mm-Mc3r-C1, Cat No. 412541; RNAscope® Probe-Cre-C2, Cat No. 312281-C2.

Slice preparation and electrophysiology

Acute brain slices were prepared in a manner similar to that described previously (Roseberry *et al.* 2007; Stuhrman & Roseberry, 2015; West & Roseberry, 2017). Briefly, adult mice were anaesthetized with isofluorane and decapitated. The brain was then removed and placed in carbogen (95% O_2 and 5% CO_2) saturated ice-cold sucrose cutting solution containing (in mM): 205 sucrose, 2.5 KCl, 0.5 $CaCl_2$, 1.25 NaH_2PO_4, 7.5 $MgCl_2$, 11.1 glucose, 21.4 $NaHCO_3$ and 0.6 kynurenic acid. A brain block containing the VTA was made, and pseudo-horizontal sections (220 μm) were cut with a vibrating blade microtome. Slices were then incubated in artificial cerebral spinal fluid (aCSF) containing (in mM): 126 NaCl, 2.5 KCl, 2.4 $CaCl_2$, 1.2 NaH_2PO_4, 1.2 $MgCl_2$, 11.1 glucose, 21.4 $NaHCO_3$ and 1 kynurenic acid at ∼35°C for 30 min and then transferred to aCSF lacking kynurenic acid for storage before recording. Slices were placed in a recording chamber and perfused with carbogen-saturated aCSF at a flow rate of ∼1–2 ml min^{-1}. Whole-cell and loose cell-attached recordings were made using an Axon multiclamp 700B microelectrode amplifier (Molecular Devices, Sunnyvale, CA, USA) and AxoGraph software (https://axograph.com). MC3R-expressing neurons were identified by the presence of EYFP using a fluorescence microscope and were patch clamped under gradient contrast optics.

Cell firing was recorded in either the loose-cell attached or whole-cell configuration. Loose cell-attached

recordings were obtained with electrodes (7.0–10.0 MΩ) filled with a Na-Hepes based internal solution containing (in mM): 135 Na-Hepes and 20 NaCl, adjusted to 290 mosmol with water. Whole-cell recordings were obtained with electrodes (2.0–3.0 MΩ) filled with a potassium gluconate (KGluconate) based internal solution containing (in mM): 128 KGluconate, 10 NaCl, 1 $MgCl_2$, 10 Hepes, 2 ATP, 0.3 GTP, 10 creatine phosphate, 10 BAPTA or 1 EGTA, and 0.1% biocytin. The internal solution contained EGTA for the experiments examining the effect of α-MSH on MC3R neuron activity under reduced calcium buffering conditions. The internal solution contained BAPTA for all other whole-cell recordings. Corrections were not made for the liquid junction potential, which was calculated for each internal solution used as: KGluconate 10 mM BAPTA, 13.9; KGluconate 1 mM EGTA, 14.7. Series resistance values were ∼3–15 MΩ. If the series resistance increased by more than 20%, the experiment was terminated or excluded from analysis. The basic action potential characteristics of VTA MC3R and non-MC3R neurons were analysed using the event detection protocol in AxoGraph. Briefly, spontaneously firing action potentials (e.g. spontaneous firing in the absence of current injection) were captured using the event detection protocol, which aligns all action potentials at threshold. The rise time (10–90%) and action potential half-width (at 50% maximum amplitude) were then obtained from the values calculated by AxoGraph and the average values were calculated for each individual cell. To measure hyperpolarization-activated cation currents (H-current), neurons were voltage clamped at –60 mV and 2 s voltage steps were applied in increasing increments of –10 mV from –50 to –100 mV with a 1 s inter-step interval. Cell firing was recorded in voltage clamp mode for loose-cell attached recordings and current clamp mode for whole-cell recordings. Whole-cell recordings were conducted in the presence of fast synaptic blockers [10 μM 6,7-dinitroquinoxaline-2,3-dione (DNQX) and 100 μM picrotoxin] and, if the cell was not firing, positive current was injected (5–55 pA). In addition, if the cell stopped firing or did not fire for at least 1 min during baseline recordings or during the first 2 min on adding the α-MSH, the experiment was terminated or excluded from the analysis. Membrane potential was recorded in current clamp mode in the presence of tetrodotoxin (1 μM, TTX). For experiments testing the effect of α-MSH on membrane current, neurons were voltage clamped at –60 mV, and slow voltage ramps were applied from –100 mV to 0 mV at 100 mV s^{-1} every 30 s in the presence of TTX. For experiments testing the effect of α-MSH on current-step evoked action potentials, the neurons were held at ∼–70 mV and 2 s current steps of 5 pA were applied at increasing amplitudes (5–50 pA) with a 1 s inter-step interval. The current-step protocol was repeated every minute and, if the current steps failed to evoke action potentials or if the number of evoked action potentials decreased over time during baseline recording, the experiment was terminated. The effects of α-MSH on all parameters (change in firing rate, membrane potential, current, or membrane resistance) were determined by averaging the baseline value for the entire 5 min prior to the addition of α-MSH, and comparing that to the average value of the 4–6 min period after the addition of α-MSH. These time points were analysed for all cells regardless of any apparent differences in the timing of the α-MSH effect between cells. For all experiments, cells were held for at least 10 min prior to drug application to allow for diffusion of the internal solution into the cell and to ensure stability of the recording prior to drug addition.

Immunohistochemistry

To identify VTA neurons used in electrophysiology experiments as dopamine or non-dopamine neurons, 0.1% biocytin was included in the internal pipette solution, and the slices were fixed and stained for TH post hoc. After the recording was terminated, the pipette was slowly removed from the neuron to allow the membrane to reseal. The brain slices were transferred to 4% paraformaldehyde and incubated at 4°C for 1–4 days, followed by washing and storage in PBS at 4°C until processing. Brain slices were then incubated with blocking buffer (5% normal goat serum, 0.2% Triton X-100, and 0.1% BSA in PBS) for 6 h at room temperature. The brain slices were then washed with PBS and incubated with a mouse monoclonal anti-TH antibody (dilution 1:1500; Millipore, Billerica, MA, USA; catalogue no. MAB318, lot no. NG1752067; RRID:AB_2201528) in antibody incubation buffer (0.2% Triton X-100 and 1% BSA in PBS) overnight at 4°C. Brain slices were washed with PBS the next day and incubated with streptavidin Alexa Fluor 594 (dilution 1:1000; Invitrogen, Carlsbad, CA, USA) and goat anti-mouse Alexa Fluor 647 (dilution 1:300, Jackson ImmunoResearch, West Grove, PA, USA) in antibody incubation buffer for 4 h at room temperature. The brain slices were then mounted to slides with gelvatol mounting media containing 10% 1,4-diazabicyclo[2.2.2]octane and imaged at 20× with a confocal microscope (LSM 700; Carl Zeiss, Oberkochen, Germany). Recorded neurons were identified as either TH-positive, TH-negative or unidentifiable. Recorded neurons positive for biocytin (red fluorescence) and TH (magenta fluorescence) were identified as TH-positive, and neurons positive for biocytin but negative for TH were identified as TH-negative. Recorded neurons were labelled as unidentifiable if the brain slice containing the recorded neuron was damaged during processing, if a biocytin labelled neuron could not be located in the brain slice, or if multiple neurons were labelled for biocytin

(which precluded the identification of the exact cell used in the experiment).

Drugs

α-MSH was purchased from Bachem (Torrance, CA, USA). TTX was purchased from Tocris Biosciences (Minneapolis, MN, USA). All other reagents were obtained from common commercial sources.

Statistical analysis

Data are represented as the mean ± SEM unless otherwise noted. Data were stored and analysed using AxoGraph X, version 1.3.5, LabChart, version 7.3.6 (ADInstruments, Sydney, NSW, Australia) and Excel, version 14.0 (Microsoft Corp. Redmond, WA, USA). Statistics were calculated using SigmaStat, version 11.0 (Systat Software, Inc., Chicago, IL, USA). To test the hypothesis that α-MSH changes the activity of VTA MC3R and non-MC3R neurons (firing rate, membrane potential, membrane resistance, rheobase, etc.), data were initially tested for normality using the Shapiro–Wilk test and were then analysed with Student's paired *t* tests, under the assumption of normality, or with Wilcoxon signed-rank tests as appropriate. To test the hypothesis that the electrical properties and action potentials of MC3R and non-MC3R VTA neurons are different, data were initially tested for normality using the Shapiro–Wilk test and were then analysed with Student's *t* tests, under the assumption of normality, or with the Mann–Whitney *U* test as appropriate. To test the hypothesis that α-MSH increases the number of current-step evoked action potentials, we used a two-way repeated measures ANOVA with Tukey's *post hoc* tests, under the assumption of normality. $P < 0.05$ was considered statistically significant *a priori*. In general, five to eight cells from five to seven mice were used in experiments examining the effects of α-MSH on VTA neuron activity.

Results

We identified MC3R-expressing VTA neurons ('VTA MC3R neurons') for electrophysiological recordings by visualizing EYFP in cells from transgenic mice that specifically express EYFP in MC3R-expressing neurons. These mice were generated by crossing mice expressing Cre recombinase in MC3R neurons (*MC3R*^{Cre}) (Pei *et al.* 2018) with a Cre inducible EYFP mouse line (Fig. 1*A*). MC3R neurons were located in the medial VTA spanning the entire anterior–posterior extent of the VTA (Fig. 1*A* and *B*). The specificity of Cre expression in MC3R-expressing neurons of *MC3R*^{Cre} mice was previously confirmed in the arcuate nucleus, ventromedial nucleus and the lateral hypothalamus (Pei *et al.* 2018). We extended this study and also tested the specificity of Cre expression in the VTA using RNAscope ISH in *MC3R*^{Cre} mice. MC3R and Cre mRNAs were also colocalized in the VTA, demonstrating that Cre is specifically expressed in MC3R-expressing neurons within the VTA of *MC3R*^{Cre} mice (Fig. 1*C–E*).

We first characterized the electrical properties of VTA MC3R neurons because VTA MC3R neurons are a novel population of VTA neurons that have not been described previously. We measured capacitance, membrane resistance and the presence of H-current in 59 MC3R neurons and 12 neighbouring non-MC3R neurons. VTA MC3R neurons had a significantly smaller capacitance (MC3R neuron, 13.27 ± 0.50 pF; Non-MC3R neuron, 23.06 ± 1.32 pF; mean difference = 9.79; $P < 0.001$; Mann–Whitney *U* test) (Fig. 2*A*) and a significantly greater membrane resistance than non-MC3R neurons (MC3R neuron, 2.12 ± 0.16 GΩ; non-MC3R neuron,

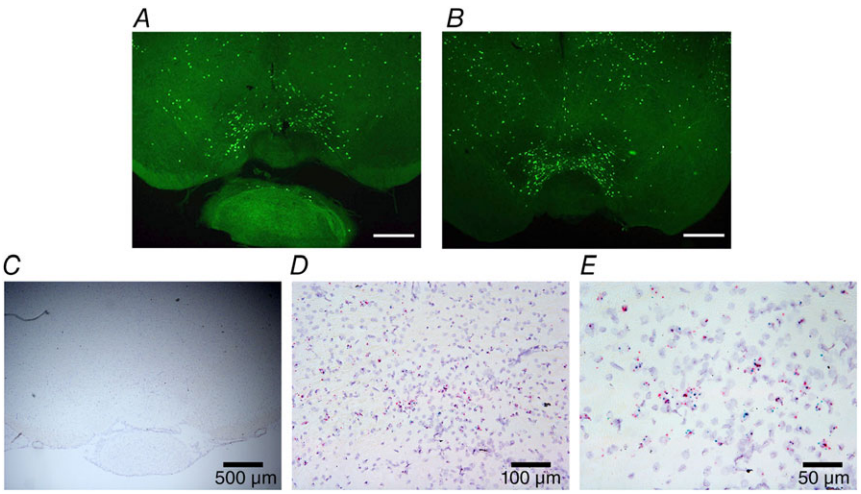

Figure 1. Expression of EYFP in MC3R neurons of the VTA from a *MC3R*^{Cre} -EYFP mouse and localization of Cre and MC3R transcripts in the VTA from a *MC3R*^{Cre} mouse
A and *B*, expression of EYFP in coronal brain slices containing the VTA from a *MC3R*^{Cre} -EYFP mouse that expresses EYFP in MC3R neurons: anterior VTA to bregma –3.28 (*A*), middle/posterior VTA to bregma –3.4 *C–E*, colocalization of MC3R mRNA (blue) and Cre mRNA (red) in coronal brain slices containing the VTA from a *MC3R*^{Cre} mouse using RNAscope ISH at 4× (*C*), 20× (*D*) and 40× (*E*). Scale bars = 500 µm (*A–C*), 100 µm (*D*) and 50 µm (*E*).

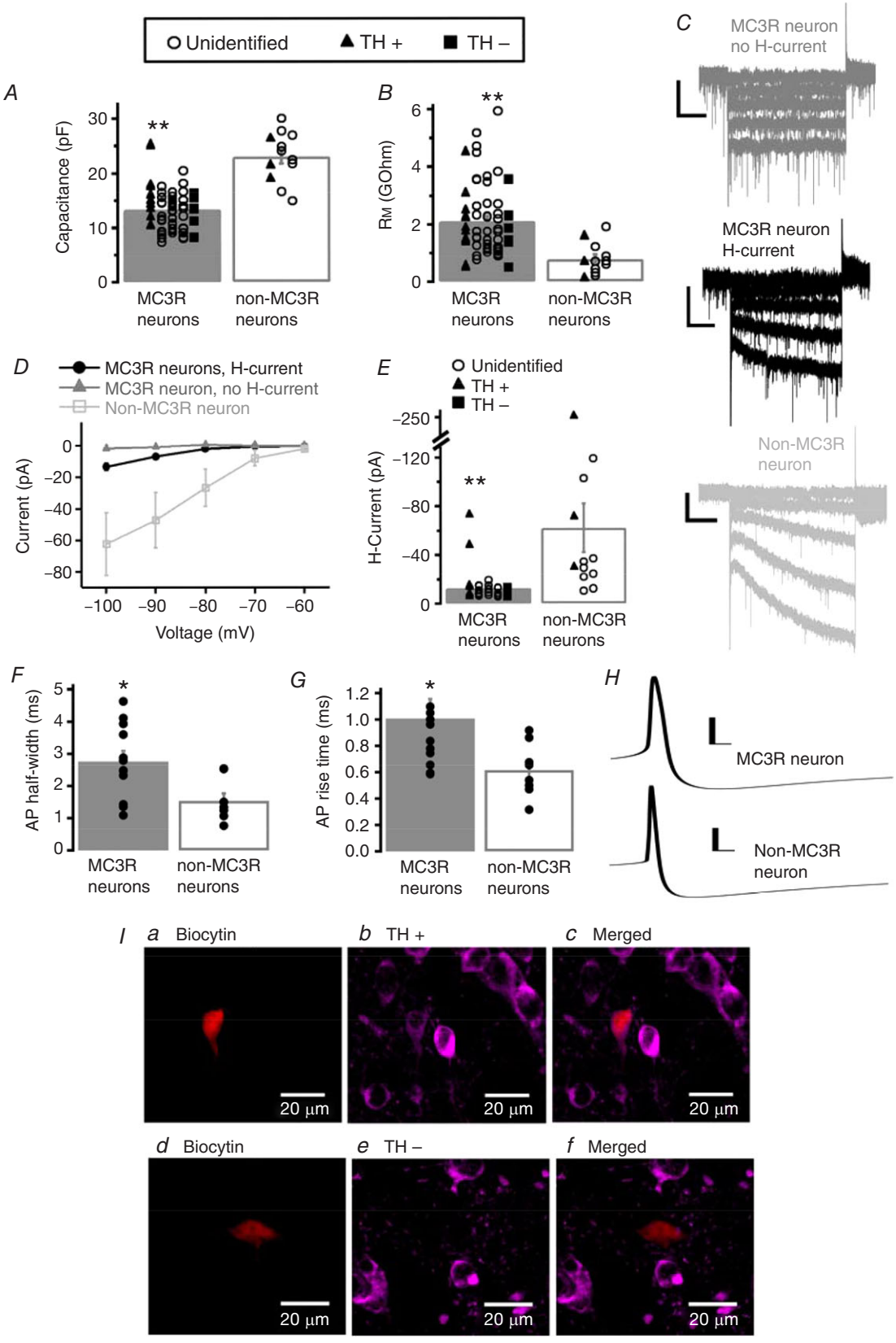

Figure 2. Characteristics of VTA MC3R neurons
A and *B*, average capacitance (*A*) and membrane resistance (R_M) (*B*) of VTA MC3R and non-MC3R neurons. *C*, sample traces from MC3R neurons without (dark grey trace) or with (black trace) H-current and a sample trace

of H-current in a non-MC3R neuron (light grey trace). *D*, average amplitude of H-current at –60, –70, –80, –90 and –100 mV for MC3R neurons without H-current, MC3R neurons with H-current and non-MC3R neurons. *E*, average amplitude of H-current at –100 mV for MC3R neurons with H-current and non-MC3R neurons. *F–G*, average action potential (AP) half-width (*F*) and rise time (*G*) of spontaneously firing VTA MC3R and non-MC3R neurons. *H*, sample traces of an action potential from a VTA MC3R and a non-MC3R neuron. *I*, example of a TH+ (*Ia–Ic*) and a TH- (*Id–If*) recorded VTA neuron. Neurons were filled with biocytin and labelled for biocytin (red, *Ia* and *Id*) and TH (magenta, *Ib* and *Ie*). Colocalization of TH and biocytin (*Ic* and *If*). MC3R neurons: $n = 59$ cells from 45 mice. Non-MC3R neurons: $n = 12$ cells from eight mice. MC3R neurons, H-current: $n = 34$ cells from 30 mice. MC3R neurons, no H-current: $n = 25$ cells from 24 mice. *F–G*, MC3R neurons: $n = 12$ cells from nine mice. Non-MC3R neurons: $n = 8$ cells from six mice. Scale bars = 30 pA 500 ms^{-1} (*C*) and 20 mV 5 ms^{-1} (*H*). $^{**}P < 0.001$ $^{*}P < 0.05$.

0.79 ± 0.16 GΩ; mean difference = 1.33; $P < 0.001$; Mann–Whitney *U* test) (Fig. 2*B*). H-current was present in 34 out of 59 of the MC3R neurons tested and was present in all 12 non-MC3R neurons tested (Fig. 2*C* and *D*). However, the H-current was significantly smaller when the cell was stepped from –60 mV to –100 mV in MC3R neurons compared to non-MC3R neurons (MC3R neuron, –13.08 ± 2.22 pA; non-MC3R neuron, –62.28 ± 19.96 pA; mean difference = 49.2; $P < 0.001$; Mann–Whitney *U* test) (Fig. 2*E*). We also examined the basic action potential characteristics of spontaneously firing MC3R and non-MC3R neurons measured with whole-cell current clamp. The average action potential height of MC3R neurons and non-MC3R neurons were 63.66 ± 2.6 mV and 64.9 ± 2.54 mV, respectively, with no significant difference between the two groups (mean difference = 1.24; $P = 0.748$; Student's *t* test). However, the action potential half-width and rise time of MC3R neurons were significantly greater than the action potential half-width and rise time of non-MC3R neurons (half-width: MC3R neuron, 2.76 ± 0.33 ms; non-MC3R neuron, 1.54 ± 0.23 ms; mean difference = 1.22; $P = 0.014$; Student's *t* test; rise time: MC3R neuron, 1.01 ± 0.15 ms; non-MC3R neuron, 0.62 ± 0.07 ms; mean difference = 0.39; $P = 0.019$; Mann–Whitney *U* test) (Fig. 2*F–H*). We filled a portion of the recorded MC3R and non-MC3R neurons with biocytin and then performed post-recording immunohistochemistry for TH to identify the recorded neurons as dopamine or non-dopamine neurons. Twelve of the 38 VTA MC3R neurons filled with biocytin were reliably identified as TH-positive and seven of the 38 were identified as TH-negative (Fig. 2*A*, *B*, *E* and *I*). Three of the eight non-MC3R neurons filled with biocytin were reliably identified as TH-positive, whereas none were identified as TH-negative (Fig. 1*A*, *B*, *E* and *I*). For both the MC3R and non-MC3R neurons, the remaining cells either could not be conclusively identified or were damaged during processing. Thus, MC3Rs are expressed in both dopamine and non-dopamine VTA neurons, and VTA MC3R neurons are smaller than non-MC3R neurons, with a higher membrane resistance, little to no H-current and broader action potentials.

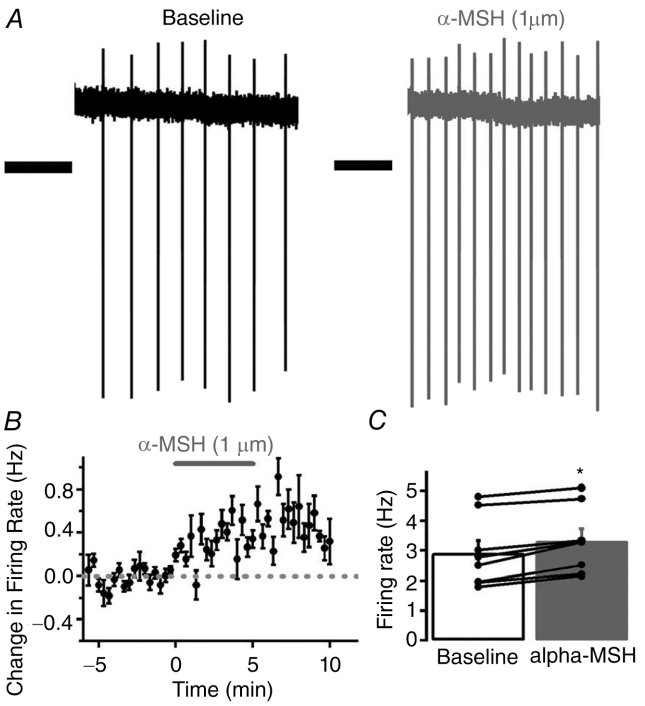

Figure 3. α-MSH increased the spontaneous firing rate of VTA MC3R neurons in loose cell-attached recordings
A, sample traces of a MC3R neuron before (black trace) and after (grey trace) α-MSH (1 μM). *B*, mean effect of α-MSH on the firing rate of MC3R neurons. *C*, mean firing rate of MC3R neurons before and after α-MSH. $n = 8$ cells from seven mice. Scale bars = 1 s. $^{*}P < 0.001$.

To determine whether α-MSH affects the activity of VTA MC3R neurons, we first tested whether α-MSH changed the spontaneous firing rate of VTA MC3R neurons in the loose-cell attached configuration. α-MSH (1 μM) significantly increased the spontaneous firing rate of VTA MC3R neurons by 0.41 ± 0.07 Hz (before α-MSH, 2.92 ± 0.41 Hz; after α-MSH, 3.33 ± 0.39 Hz; $P < 0.001$; Student's paired *t* test) (Fig. 3). Out of the eight MC3R neurons tested, all exhibited an action potential width ≥1.2 ms, suggesting that the MC3R neurons tested were dopaminergic. A broad action potential width is a physiological characteristic that is indicative of dopamine neurons and has repeatedly and reliably been used to identify dopamine neurons in cell-attached and extracellular recordings (Ungless *et al.* 2004; Ford *et al.* 2006; Chieng *et al.* 2011). However, we could

not use post-recording immunohistochemistry to identify dopamine neurons in these experiments and, without validation, cannot conclusively classify these neurons as dopaminergic. Thus, α-MSH increases the firing of VTA putative dopamine neurons expressing MC3Rs.

We next confirmed and extended these findings by testing whether α-MSH increases the firing rate of VTA MC3R neurons in the whole-cell current clamp configuration. We included blockers of fast synaptic currents (10 μM DNQX, 100 μM picrotoxin) in the bath solution to confirm that the α-MSH induced increase in MC3R neuron firing rate was a result of a direct action on MC3Rs and not changes in synaptic transmission. α-MSH (1 μM) significantly increased the firing rate of MC3R neurons by 0.42 $\pm$ 0.11 Hz in the presence of fast synaptic blockers (before α-MSH, 1.17 $\pm$ 0.21 Hz; after α-MSH, 1.59 $\pm$ 0.15 Hz; $P = 0.012$; Student's paired t test) (Fig. 4*A*–*C*). Intracellular Ca^{2+} plays a key role in VTA dopamine neuron excitability, firing rate and burst firing (Grace & Bunney, 1984*b*, a; Paladini & Roeper, 2014) and so we next tested whether reduced Ca^{2+} buffering affected the α-MSH induced increase in MC3R neuron firing rate using an internal solution containing a low Ca^{2+} buffer (1 mM EGTA). α-MSH (1 μM) also significantly increased the firing rate of MC3R neurons using the 1 mM EGTA internal solution by 0.51 $\pm$ 0.17 Hz (before α-MSH, 1.28 $\pm$ 0.34 Hz; after α-MSH, 1.78 $\pm$ 0.47 Hz; $P = 0.028$; Student's paired t test) (Fig. 4*D* and *E*), with no significant difference between the magnitudes of α-MSH induced increase in firing rate between the two groups (10 mM BAPTA, 0.42 $\pm$ 0.11 Hz *vs.* 1 mM EGTA, 0.51 $\pm$ 0.17 Hz; mean difference = 0.09; $P = 0.673$; Student's t test). Thus,

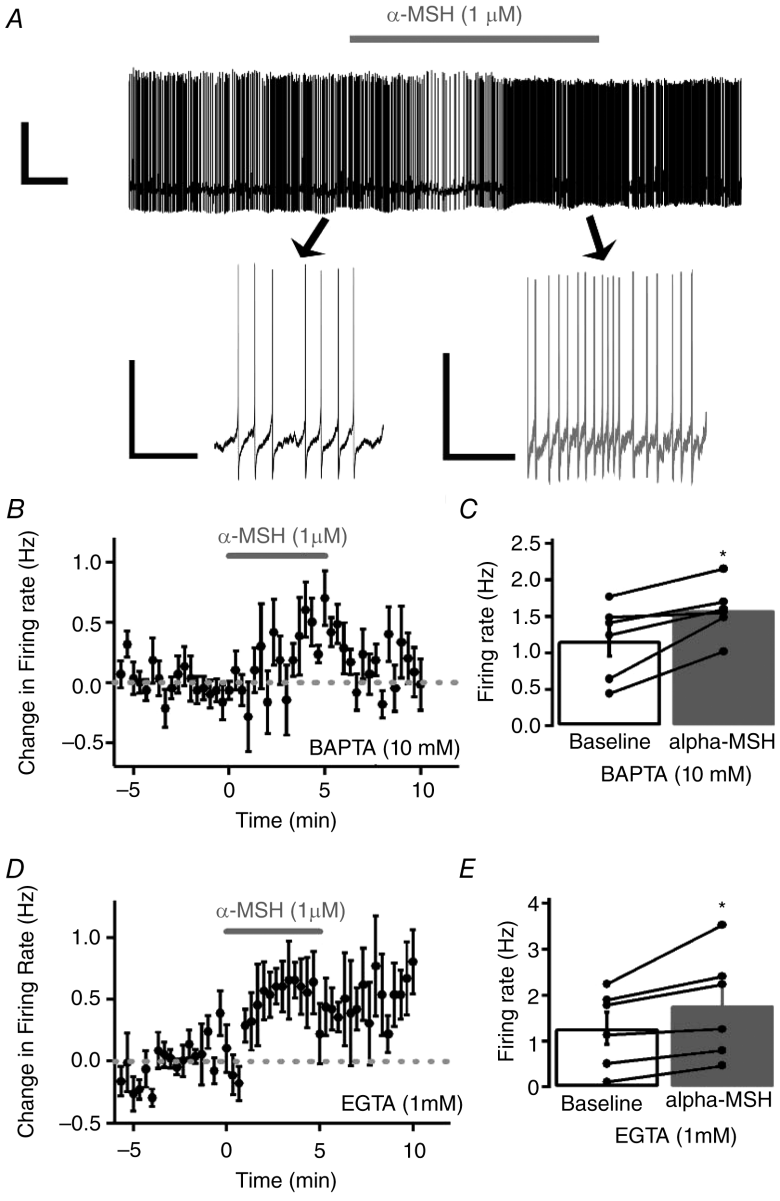

Figure 4. α-MSH increased the firing rate of VTA MC3R neurons in whole-cell current clamp recordings in the presence of inhibitors of fast synaptic transmission (DNQX: 10 μm; picrotoxin: 100 μm)
A, sample traces of the firing rate of a MC3R neuron before (black trace), during and after (grey trace) α-MSH (1 μM) application. *B* and *D*, mean effect of α-MSH on the firing rate of MC3R neurons using an internal solution containing 10 mM BAPTA (*B*) or 1 mM EGTA (*D*). *C* and *E*, mean firing rate of MC3R neurons before and after α-MSH using an internal solution containing 10 mM BAPTA (*C*) or 1 mM EGTA (*E*). $n = 6$ cells from six mice for each group. Scale bars = 40 mV min^{-1} (top trace) and 40 mV 4 s^{-1} (bottom trace). *$P < 0.05$.

α-MSH increases the firing rate of VTA MC3R neurons via a mechanism independent of fast synaptic transmission and intracellular Ca^{2+} levels. To identify whether these MC3R neurons were dopaminergic, we labelled the MC3R neurons with biocytin and stained for TH. Five out of 12 were TH-positive and we were unable to reliably identify the remaining seven neurons. These experiments further confirm that α-MSH increases the firing rate of VTA dopamine neurons expressing MC3Rs.

MC3Rs are only expressed in a subset of VTA neurons (Lippert *et al.* 2014) and there is some low level expression of MC4Rs in the VTA (Roselli-Rehfuss *et al.* 1993; Liu *et al.* 2003; Lippert *et al.* 2014) and so we next tested whether the α-MSH induced increase in VTA MC3R neuron firing rate was specific to VTA MC3R neurons. In these experiments, we tested the effect of α-MSH on non-MC3R neuron activity under the exact same conditions used to test the effect of α-MSH on MC3R neuron activity (e.g. in whole-cell current clamp configuration with blockers of fast synaptic currents) (Fig. 4*C*). α-MSH did not increase the firing rate of non-MC3R expressing VTA neurons (before α-MSH, 0.70 ± 0.14 Hz, after α-MSH: 0.49 ± 0.13 Hz; $P = 0.104$; Student's paired t test) (Fig. 5). There was a trend toward a decrease in firing rate (–0.2 ± 0.11 Hz), although this decrease was not statistically significant (Fig. 5*C*). The non-MC3R neurons tested were stained for TH, and three out of five neurons tested were TH-positive, whereas 2 could not reliably be identified. Therefore, α-MSH does not increase the firing rate of non-MC3R expressing dopamine neurons and the α-MSH induced increase in VTA neuron firing appears to be specific to VTA MC3R neurons.

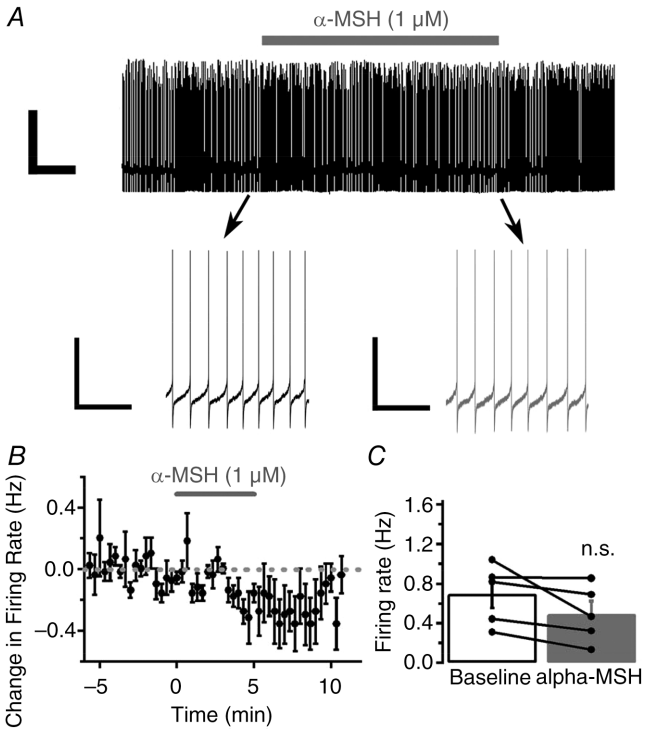

Figure 5. α-MSH did not increase the firing rate of non-MC3R expressing VTA neurons in whole-cell current clamp recordings in the presence of inhibitors of fast synaptic transmission (DNQX: 10 μm; picrotoxin: 100 μm)
A, sample traces of the firing rate of a non-MC3R neuron before (black trace), during and after (grey trace) α-MSH (1 μM) application. *B*, mean effect of α-MSH on the firing rate of non-MC3R neurons. *C*, mean firing rate of non-MC3R neurons before and after α-MSH. $n = 5$ cells from five mice. Scale bars = 50 mV min^{-1} (top trace) and 40 mV 4 s^{-1} (bottom trace). n.s., not significant.

α-MSH could increase the activity of VTA MC3R neurons by direct depolarization or by modifying the firing properties of the cell (e.g. threshold) independent of a direct change in membrane potential. To determine whether α-MSH directly depolarizes MC3R neurons, we tested the effect of α-MSH on membrane potential in the presence of TTX (1 μM), DNQX (10 μM) and picrotoxin (100 μM). α-MSH (1 μM) slightly increased the membrane potential of MC3R neurons, although this increase was not statistically significant (before α-MSH, –53.7 ± 3.7 mV; after α-MSH –52.4 ± 3.6 mV; mean depolarization = 1.34 ± 0.84 mV; $P = 0.177$; Student's paired t test) (Fig. 6*A* and *B*). To confirm and extend our results, we used voltage clamp to test the effect of α-MSH on membrane current and slow voltage ramps (–100 mV to 0 mV 100 mV s^{-1}) in the presence of TTX (1 μM), DNQX (10 μM) and picrotoxin (100 μM). α-MSH (1 μM) did not affect membrane current or membrane resistance in VTA MC3R neurons (R_M before α-MSH, 1413.61 ± 292.72 MΩ; R_M after α-MSH 1276.18 ± 210.7 MΩ; mean difference = 137.43; $P = 0.156$; Wilcoxin signed-rank test) (Fig. 6*C* and *D*). The MC3R neurons tested in these experiments were also stained for TH, and four out of 12 were TH-positive, three were TH-negative and five could not be reliably identified.

We then tested whether α-MSH altered VTA MC3R neuron firing independent of a direct depolarization by testing the effect of α-MSH on current-step evoked action potentials. The neurons were held at ∼–70 mV and a set of current steps of increasing amplitude (5–50 pA in 5 pA increments; 2 s each; 1 s inter-step interval) were applied every minute. α-MSH (1 μM) did not significantly affect rheobase (i.e. the minimal current required to reach threshold potential and generate an action potential) (before α-MSH, 26.9 ± 3.5 pA; after α-MSH, 25 ± 3 pA; mean difference = 1.9; $P = 0.351$; Student's paired t test) (Fig. 7*B* and *E*) or membrane potential (before α-MSH, –70.6 ± 0.87 mV; after α-MSH, –68.1 ± 1.7 mV; mean difference = 2.5; $P = 0.181$; Student's paired t test) (Fig. 7*C* and *D*). However, α-MSH (1 μM) did significantly increase the number of current-evoked action potentials at the 35, 40, 45 and 50 pA current steps in MC3R neurons (significant main effect of current step, $F_{9,63} = 22.135$, $P < 0.001$) (Fig. 7*A*

and *B*) and significant current-step × α-MSH interaction ($F_{9,63} = 3.227$, $P = 0.003$; two-way repeated measures ANOVA). The current-step evoked action potentials were further analysed at the 40 pA current step because this step consistently evoked three or four action potentials at baseline in seven out of eight neurons tested. One cell was excluded from this analysis because the 40 pA current step failed to consistently evoke action potentials. α-MSH significantly decreased the inter-spike interval at the 40 pA current step (before α-MSH, 119.7 ± 20.8 ms; after α-MSH, 90.9 ± 12.1 ms; mean difference = 28.8; $P = 0.016$; Wilcoxin signed-rank test) (Fig. 7*F*) and there was a trend towards a decrease in the latency to the first spike at the 40 pA current step (before α-MSH, 1.07 ± 0.13 s; after α-MSH, 0.85 ± 0.07 s; mean difference = 0.22; $P = 0.131$; Student's paired *t* test) (Fig. 7*G*). Thus, α-MSH facilitates MC3R neuron firing via an activity-dependent mechanism that does not appear to involve direct depolarization or a change in rheobase or threshold potential. Consistent with our other experiments, we stained these MC3R neurons for TH, and one out of eight were identified as TH-positive, four as TH-negative and three could not be reliably identified. Thus, these results suggest α-MSH increases the firing rate of both dopamine and non-dopamine VTA MC3R neurons.

Discussion

In these studies, we have shown that α-MSH significantly increases the firing rate of VTA MC3R neurons via an activity-dependent mechanism because α-MSH increased the activity of MC3R neurons only when the neurons were firing. α-MSH did slightly increase the membrane potential of MC3R neurons; therefore, it is possible that this slight increase in membrane potential caused a significant increase in MC3R neuron firing. In addition, α-MSH did not affect rheobase in MC3R neurons, suggesting that α-MSH does not increase the firing rate of MC3R neurons by lowering threshold potential. Furthermore, α-MSH increased the firing rate via a mechanism independent of fast synaptic transmission and intracellular Ca^{2+} levels. Thus, our results suggest α-MSH increases the firing rate of VTA MC3R neurons via an activity-dependent mechanism that is independent of intracellular Ca^{2+} levels or altered synaptic transmission onto VTA MC3R neurons.

The VTA comprises a heterogeneous population of neurons including dopamine, GABA and glutamate neurons that have different projection targets, electrophysiological characteristics and molecular markers (Morales & Margolis, 2017). We examined the electrophysiological characteristics of VTA MC3R neurons and found that they had a significantly smaller capacitance compared to non-MC3R neurons, suggesting that MC3R neurons are smaller than non-MC3R neurons. In addition, VTA MC3R neurons had a significantly higher membrane resistance, little to no H-current, and a greater action potential half-width and rise time compared to non-MC3R neurons. Previous studies have shown that the highest levels of VTA MC3R neurons are found in the ventromedial region of the VTA (Lippert *et al.*

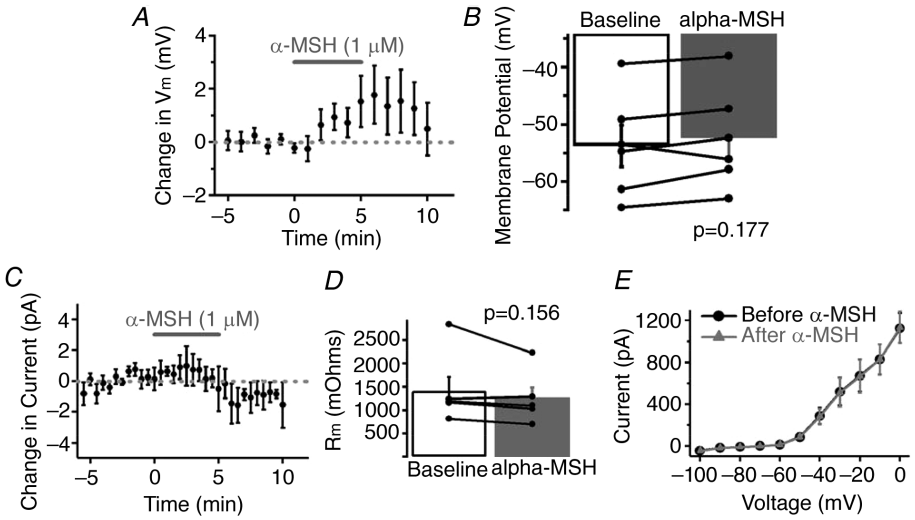

Figure 6. α-MSH did not significantly affect the membrane potential, current, or resistance of VTA MC3R neurons in the presence of TTX (1 μm)
A, mean effect of α-MSH (1 μM) on the membrane potential of MC3R neurons. *B*, mean membrane potential of MC3R neurons before and after α-MSH. *C*, mean effect of α-MSH (1 μM) on membrane current of MC3R neurons. *D*, mean membrane resistance (R_M) of MC3R neurons before and after α-MSH. *E*, mean effect of α-MSH on slow voltage ramps (–100 mV to 0 mV 100 mV s^{-1}) before (black trace) and after α-MSH (1 μM; grey trace) in MC3R neurons. $n = 6$ cells from five mice for each group.

2014), and for our experiments, recorded VTA MC3R neurons were located in more medial regions of the VTA, whereas recorded non-MC3R neurons were located in the central to more lateral regions of the VTA. Our results and the location of MC3R neurons suggests that VTA dopamine neurons expressing MC3Rs probably project to the medial PFC (mPFC), NAc core, NAc medial shell or basolateral amygdala because VTA dopamine neurons projecting to these areas are significantly smaller than dopamine neurons projecting to the NAc lateral shell and are primarily located in the medial posterior VTA (Lammel *et al.* 2008). Furthermore, it was previously shown that VTA dopamine neurons projecting to the basolateral amygdala and NAc medial shell have a significantly smaller capacitance, higher membrane resistance and little to no H-current compared to NAc lateral shell projecting dopamine neurons (Baimel *et al.* 2017). In addition, mPFC, NAc core, NAc medial shell and basolateral amygdala projecting VTA dopamine neurons have wider action potentials compared to the action potentials of NAc lateral shell projecting dopamine neurons (Lammel *et al.* 2008; Baimel *et al.* 2017). Thus, the electrical properties of VTA MC3R neurons suggest that dopamine neurons expressing MC3Rs most probably project to the mPFC, NAc core, NAc medial shell, or basolateral amygdala and do not project to the NAc lateral shell, although further experiments are needed to determine the projection targets of VTA MC3R neurons.

MC3Rs are expressed in both VTA dopamine and non-dopamine neurons (dopamine: ∼57%; non-dopamine: ∼43%) (Lippert *et al.* 2014). The identity of MC3R non-dopamine neurons is currently unknown and these neurons may be GABAergic or glutamatergic neurons because both are found in the

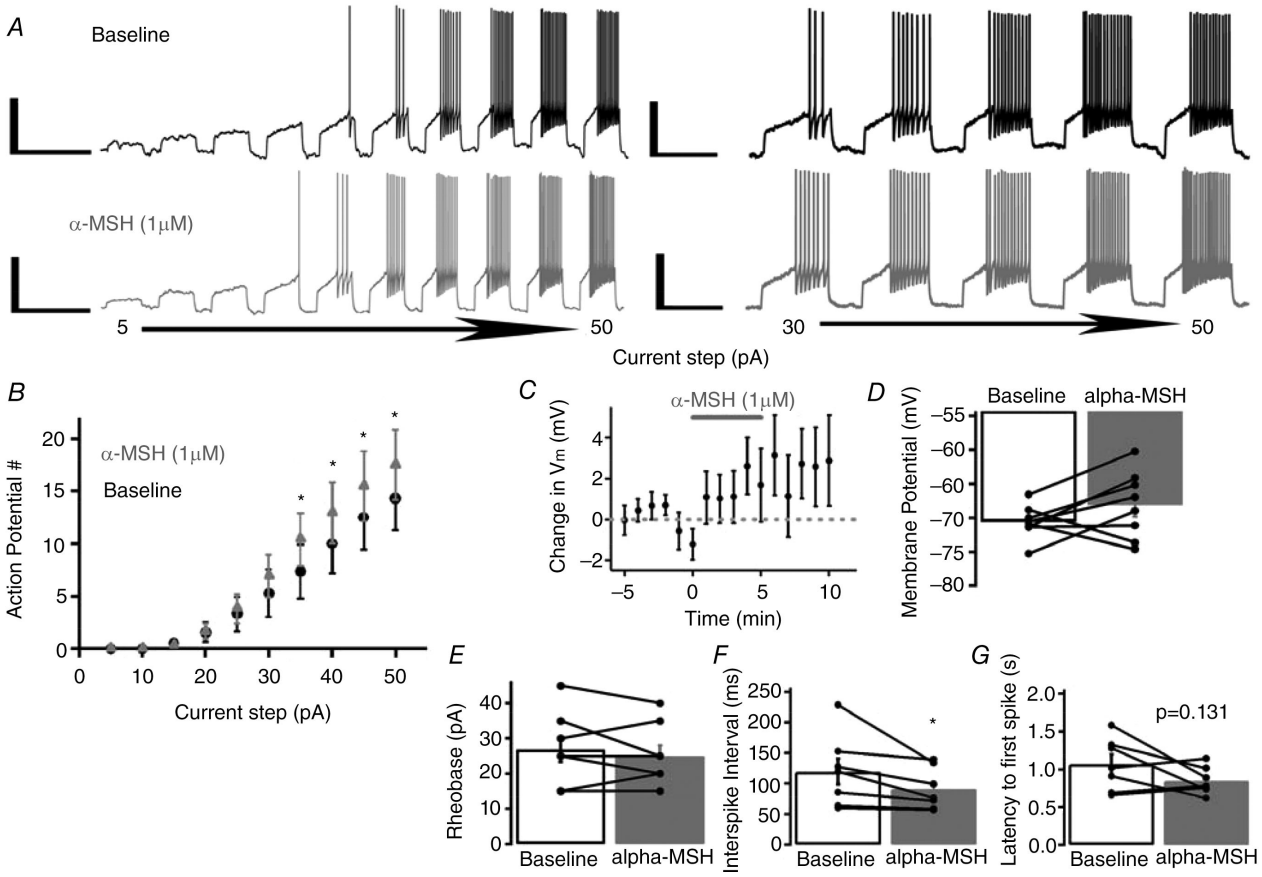

Figure 7. α-MSH increased the number of current-step evoked action potentials but did not affect rheobase in VTA MC3R neurons
Current steps (2 s) of increasing amplitude (5–50 pA) were applied every minute before, during and after α-MSH (1 μM) application. *A*, sample traces of a MC3R neuron before (black trace) and after (grey trace) α-MSH. *B*, mean effect of α-MSH on the number of action potentials evoked by incrementing 5 pA current-steps (5–50 pA). *C* and *D*, mean effect of α-MSH on membrane potential (*C*) and mean membrane potential before and after α-MSH (*D*) for the MC3R neurons in (*B*). *E* and *G*, mean rheobase (the minimum current step required to initiate an action potential) (*E*), mean inter-spike interval at the 40 pA step (*F*) and mean latency to the first spike at the 40 pA step (*G*) before and after α-MSH. n = 7–8 cells from six or seven mice for each group. Scale bars = 40 mV 5 s^{-1} (left traces) and 40 mV 2 s^{-1} (right traces). $^*P < 0.05$.

VTA (Yamaguchi *et al.* 2007; Nair-Roberts *et al.* 2008; Margolis *et al.* 2012). Previous studies have shown that intra-VTA α-MSH increases dopamine release in the NAc and dopamine-dependent behaviours, suggesting that α-MSH increases VTA dopamine neuron activity (Torre & Celis, 1986, 1988; Klusa *et al.* 1999; Lindblom *et al.* 2001; Sanchez *et al.* 2001; Jansone *et al.* 2004). In addition, γ-MSH increased the firing rate of a subset of VTA dopamine neurons in rats (Pandit *et al.* 2016). In agreement, our results suggest that α-MSH increases the firing rate of VTA dopamine neurons expressing MC3Rs. All of the MC3R neurons tested in the cell-attached recordings had broad action potential widths ($\geq$1.2 ms), which has been shown to reliably identify mouse VTA dopamine neurons in cell-attached recordings (Ford *et al.* 2006; Chieng *et al.* 2011), suggesting that the neurons recorded in our cell-attached experiments are putative dopamine neurons. In addition, 12 of the MC3R neurons tested in our experiments were TH positive. Nevertheless, our results also suggest that α-MSH increases the firing rate of VTA non-dopamine MC3R neurons because seven MC3R neurons were TH negative. Thus, α-MSH probably increases the firing rate of dopamine and non-dopamine VTA MC3R neurons. In conclusion, we have shown that α-MSH increases the firing rate of VTA dopamine MC3R-expressing neurons, although α-MSH may increase the firing rate of VTA GABA and/or glutamate MC3R-expressing neurons as well, and further studies will be required to conclusively identify the specific subtypes of VTA MC3R neurons responding to α-MSH.

Altering VTA dopamine neuron activity and downstream dopamine release affects food intake and feeding behaviour, although how VTA dopamine neuron activity regulates feeding behaviour is complex and not completely understood (Palmiter, 2007; Kenny, 2011; Volkow *et al.* 2011). For example, increasing dopamine neuron activity and dopamine release can both increase and decrease food intake. Indeed, increasing dopamine release in the NAc using a low dose of amphetamine increases food intake, whereas higher doses decrease food intake in rats (Evans & Vaccarino, 1986) and anorexigenic (feeding inhibiting) and orexigenic (feeding stimulating) peptides have both been shown to increase dopamine neuron activity, although having opposite effects on food intake (Liu & Borgland, 2015). Furthermore, different anorexigenic peptides decrease food intake by either increasing or decreasing dopamine neuron activity and dopamine release depending on the peptide (Liu & Borgland, 2015). For example, the anorexigenic peptides insulin and leptin decrease dopamine neuron activity and feeding (Hommel *et al.* 2006; Labouebe *et al.* 2013; Thompson & Borgland, 2013), although α-MSH increases NAc dopamine release (Torre & Celis, 1986, 1988; Lindblom *et al.* 2001; Sanchez *et al.* 2001; Jansone *et al.* 2004) and decreases feeding (Roseberry, 2013; Yen & Roseberry, 2015; Shanmugarajah *et al.* 2017). However, it was previously unknown how α-MSH increased NAc dopamine release at the cellular level to regulate feeding behaviour. In the present study, we have identified a novel mechanism for the control of VTA MC3R neuron activity by α-MSH. As a result, these studies provide a better understanding of how α-MSH acts in the VTA at the cellular level and suggest that intra-VTA α-MSH decreases food intake and food reward by increasing the activity of a specific population of VTA dopamine and non-dopamine neurons via an activity-dependent mechanism.

The effect of α-MSH on VTA MC3R neurons probably occurs via activation of MC3Rs because MC3Rs are highly expressed in the VTA (Roselli-Rehfuss *et al.* 1993; Lippert *et al.* 2014). It is possible that α-MSH could mediate its effect on MC3R neurons by acting on MC4Rs as well, although this appears to be improbable. Although MC4Rs are also expressed in the VTA, they are expressed at much lower levels compared to MC3Rs (Roselli-Rehfuss *et al.* 1993; Liu *et al.* 2003; Lippert *et al.* 2014) and MC4Rs are most abundantly expressed in caudal regions of the VTA, whereas MC3Rs are expressed throughout the rostral-caudal extent of the VTA (Lippert *et al.* 2014). Thus, although we cannot rule out the possibility that the effects of α-MSH on VTA MC3R neuron activity are also mediated by MC4Rs in some of the MC3R neurons tested, this appears to be improbable.

We also showed that α-MSH does not significantly increase the firing rate of non-MC3R expressing VTA neurons, although there was a trend toward a decrease in firing rate in these studies because α-MSH reduced the firing rate of four out of five of the non-MC3R neurons tested. This decrease in firing rate may be a result of run down because the firing rate slowly ran down in most of the recorded neurons. Alternatively, α-MSH may decrease the firing rate of non-MC3R expressing VTA dopamine neurons via activation of dopamine D2 receptors. VTA dopamine neurons release dopamine from their soma and dendrites (Bjorklund & Lindvall, 1975; Geffen *et al.* 1976; Kalivas & Duffy, 1991; Rice *et al.* 1997; Beckstead *et al.* 2004) and this somatodendritic release inhibits neighbouring dopamine neurons via dopamine D2 receptor-mediated activation of G-coupled inward rectifying potassium channels (Aghajanian & Bunney, 1977; Lacey *et al.* 1987; Mercuri *et al.* 1997; Beckstead *et al.* 2004). Our results suggest α-MSH increases the firing rate of VTA dopamine-MC3R neurons and so the increased activity of dopamine-MC3R neurons could have caused an increase in somatodendritic dopamine release and inhibition of neighbouring VTA dopamine neurons, although this possibility remains to be tested.

The exact mechanisms by which α-MSH increases VTA MC3R neuron activity are unknown. MC3Rs

are G protein-coupled receptors that signal via G_s and thus activate adenylyl cyclase and subsequently cAMP and protein kinase A (PKA) (Roselli-Rehfuss *et al.* 1993). However, additional experiments have demonstrated that the MC3R is coupled to other G-proteins and can activate other signalling pathways. For example, activating MC3Rs in HEK293 cells also activates mitogen-activated protein kinase (MAPK) via a Gi protein-phosphoinositide 3-kinase signalling pathway (Chai *et al.* 2007). Thus, it is possible that α-MSH increases VTA MC3R neuron activity by activating PKA, MAPK or phosphoinositide 3-kinase and subsequently increasing or decreasing the conductance of an ion channel current via its phosphorylation. Indeed, reducing M-current (a voltage-gated potassium current) in VTA dopamine neurons significantly decreases the inter-spike interval of evoked action potentials (Koyama & Appel, 2006) and blocking A-type current (a low-threshold voltage-gated potassium current) increases the firing rate and the inward inter-spike current in VTA dopamine neurons (Khaliq & Bean, 2008). Thus, α-MSH could increase the firing rate of VTA MC3R neurons by reducing M-current or A-type current because α-MSH did significantly decrease the inter-spike interval of evoked action potentials in VTA MC3R neurons. In addition, α-MSH could increase the firing rate of MC3R neurons by increasing the conductance of a Na^+ current because spontaneous firing in VTA dopamine neurons is primarily dependent on two Na^+ currents: a TTX insensitive Na^+ leak current and a TTX-sensitive voltage-dependent Na^+ current (Khaliq & Bean, 2010; Gantz *et al.* 2018). Finally, it is also possible that α-MSH directly increases VTA MC3R neuron activity simply via direct depolarization because α-MSH did slightly depolarize MC3R neurons, although this change in membrane potential was not statistically significant, making it difficult to determine the contribution of this change to the observed increase in firing. Thus, further experiments are needed to determine how α-MSH increases VTA MC3R neuron firing rate, as well as to identify the intracellular signalling pathway mediating these effects.

In summary, we have shown that α-MSH increases the firing rate of MC3R expressing VTA neurons via an activity-dependent mechanism. These results advance our understanding of the cellular mechanisms by which intra-VTA α-MSH regulates food intake, food reward and other dopamine-dependent behaviours, as well as how intra-VTA α-MSH increases dopamine turnover in the NAc.

References

Afshin A, Forouzanfar MH, Reitsma MB, Sur P, Estep K, Lee A, Marczak L, Mokdad AH, Moradi-Lakeh M, Naghavi M, Salama JS, Vos T, Abate KH, Abbafati C, Ahmed MB, Al-Aly Z, Alkerwi A, Al-Raddadi R, Amare AT, Amberbir A, Amegah AK, Amini E, Amrock SM, Anjana RM, Arnlov J, Asayesh H, Banerjee A, Barac A, Baye E, Bennett DA, Beyene AS, Biadgilign S, Biryukov S, Bjertness E, Boneya DJ, Campos-Nonato I, Carrero JJ, Cecilio P, Cercy K, Ciobanu LG, Cornaby L, Damtew SA, Dandona L, Dandona R, Dharmaratne SD, Duncan BB, Eshrati B, Esteghamati A, Feigin VL, Fernandes JC, Furst T, Gebrehiwot TT, Gold A, Gona PN, Goto A, Habtewold TD, Hadush KT, Hafezi-Nejad N, Hay SI, Horino M, Islami F, Kamal R, Kasaeian A, Katikireddi SV, Kengne AP, Kesavachandran CN, Khader YS, Khang YH, Khubchandani J, Kim D, Kim YJ, Kinfu Y, Kosen S, Ku T, Defo BK, Kumar GA, Larson HJ, Leinsalu M, Liang X, Lim SS, Liu P, Lopez AD, Lozano R, Majeed A, Malekzadeh R, Malta DC, Mazidi M, McAlinden C, McGarvey ST, Mengistu DT, Mensah GA, Mensink GBM, Mezgebe HB, Mirrakhimov EM, Mueller UO, Noubiap JJ, Obermeyer CM, Ogbo FA, Owolabi MO, Patton GC, Pourmalek F, Qorbani M, Rafay A, Rai RK, Ranabhat CL, Reinig N, Safiri S, Salomon JA, Sanabria JR, Santos IS, Sartorius B, Sawhney M, Schmidhuber J, Schutte AE, Schmidt MI, Sepanlou SG, Shamsizadeh M, Sheikhbahaei S, Shin MJ, Shiri R, Shiue I, Roba HS, Silva DAS, Silverberg JI, Singh JA, Stranges S, Swaminathan S, Tabares-Seisdedos R, Tadese F, Tedla BA, Tegegne BS, Terkawi AS, Thakur JS, Tonelli M, Topor-Madry R, Tyrovolas S, Ukwaja KN, Uthman OA, Vaezghasemi M, Vasankari T, Vlassov VV, Vollset SE, Weiderpass E, Werdecker A, Wesana J, Westerman R, Yano Y, Yonemoto N, Yonga G, Zaidi Z, Zenebe ZM, Zipkin B & Murray CJL (2017). Health effects of overweight and obesity in 195 countries over 25 years. *N Engl J Med* **377**, 13–27.

Aghajanian GK & Bunney BS (1977). Dopamine 'autoreceptors': pharmacological characterization by microiontophoretic single cell recording studies. *Naunyn Schmiedebergs Arch Pharmacol* **297**, 1–7.

Aponte Y, Atasoy D & Sternson SM (2011). AGRP neurons are sufficient to orchestrate feeding behavior rapidly and without training. *Nat Neurosci* **14**, 351–355.

Baimel C, Lau BK, Qiao M & Borgland SL (2017). Projection-target-defined effects of orexin and dynorphin on VTA dopamine neurons. *Cell Rep* **18**, 1346–1355.

Beckstead MJ, Grandy DK, Wickman K & Williams JT (2004). Vesicular dopamine release elicits an inhibitory postsynaptic current in midbrain dopamine neurons. *Neuron* **42**, 939–946.

Beninger RJ, Cheng M, Hahn BL, Hoffman DC, Mazurski EJ, Morency MA, Ramm P & Stewart RJ (1987). Effects of extinction, pimozide, SCH 23390, and metoclopramide on food-rewarded operant responding of rats. *Psychopharmacology (Berl)* **92**, 343–349.

Bjorklund A & Lindvall O (1975). Dopamine in dendrites of substantia nigra neurons: suggestions for a role in dendritic terminals. *Brain Res* **83**, 531–537.

Chai B, Li JY, Zhang W, Ammori JB & Mulholland MW (2007). Melanocortin-3 receptor activates MAP kinase via PI3 kinase. *Regul Pept* **139**, 115–121.

Chieng B, Azriel Y, Mohammadi S & Christie MJ (2011). Distinct cellular properties of identified dopaminergic and GABAergic neurons in the mouse ventral tegmental area. *J Physiol* **589**, 3775–3787.

Cousins MS, Wei W & Salamone JD (1994). Pharmacological characterization of performance on a concurrent lever pressing/feeding choice procedure: effects of dopamine antagonist, cholinomimetic, sedative and stimulant drugs. *Psychopharmacology (Berl)* **116**, 529–537.

Dietrich MO, Bober J, Ferreira JG, Tellez LA, Mineur YS, Souza DO, Gao XB, Picciotto MR, Araujo I, Liu ZW & Horvath TL (2012). AgRP neurons regulate development of dopamine neuronal plasticity and nonfood-associated behaviors. *Nat Neurosci* **15**, 1108–1110.

Evans KR & Vaccarino FJ (1986). Intra-nucleus accumbens amphetamine: dose-dependent effects on food intake. *Pharmacol Biochem Behav* **25**, 1149–1151.

Fan W, Boston BA, Kesterson RA, Hruby VJ & Cone RD (1997). Role of melanocortinergic neurons in feeding and the agouti obesity syndrome. *Nature* **385**, 165–168.

Finkelstein EA, Ruhm CJ & Kosa KM (2005). Economic causes and consequences of obesity. *Annu Rev Public Health* **26**, 239–257.

Ford CP, Mark GP & Williams JT (2006). Properties and opioid inhibition of mesolimbic dopamine neurons vary according to target location. *J Neurosci* **26**, 2788–2797.

Gantz SC, Ford CP, Morikawa H & Williams JT (2018). The evolving understanding of dopamine neurons in the substantia nigra and ventral tegmental area. *Annu Rev Physiol* **80**, 219–241.

Geffen LB, Jessell TM, Cuello AC & Iversen LL (1976). Release of dopamine from dendrites in rat substantia nigra. *Nature* **260**, 258–260.

Grace AA & Bunney BS (1984*a*). The control of firing pattern in nigral dopamine neurons: burst firing. *J Neurosci* **4**, 2877–2890.

Grace AA & Bunney BS (1984*b*). The control of firing pattern in nigral dopamine neurons: single spike firing. *J Neurosci* **4**, 2866–2876.

Grundy D (2015). Principles and standards for reporting animal experiments in The Journal of Physiology and Experimental Physiology. *J Physiol* **593**, 2547–2549.

Hahn TM, Breininger JF, Baskin DG & Schwartz MW (1998). Coexpression of Agrp and NPY in fasting-activated hypothalamic neurons. *Nat Neurosci* **1**, 271–272.

Hall KD, Guo J, Dore M & Chow CC (2009). The progressive increase of food waste in America and its environmental impact. *PLoS ONE* **4**, e7940.

Hommel JD, Trinko R, Sears RM, Georgescu D, Liu ZW, Gao XB, Thurmon JJ, Marinelli M & DiLeone RJ (2006). Leptin receptor signaling in midbrain dopamine neurons regulates feeding. *Neuron* **51**, 801–810.

Jansone B, Bergstrom L, Svirskis S, Lindblom J, Klusa V & Wikberg JE (2004). Opposite effects of gamma(1)- and gamma(2)-melanocyte stimulating hormone on regulation of the dopaminergic mesolimbic system in rats. *Neurosci Lett* **361**, 68–71.

Kalivas PW & Duffy P (1991). A comparison of axonal and somatodendritic dopamine release using in vivo dialysis. *J Neurochem* **56**, 961–967.

Kenny PJ (2011). Reward mechanisms in obesity: new insights and future directions. *Neuron* **69**, 664–679.

Khaliq ZM & Bean BP (2008). Dynamic, nonlinear feedback regulation of slow pacemaking by A-type potassium current in ventral tegmental area neurons. *J Neurosci* **28**, 10905–10917.

Khaliq ZM & Bean BP (2010). Pacemaking in dopaminergic ventral tegmental area neurons: depolarizing drive from background and voltage-dependent sodium conductances. *J Neurosci* **30**, 7401–7413.

King CM & Hentges ST (2011). Relative number and distribution of murine hypothalamic proopiomelanocortin neurons innervating distinct target sites. *PLoS ONE* **6**, e25864.

Klusa V, Svirskis S, Opmane B, Muceniece R & Wikberg JE (1999). Behavioural responses of gamma-MSH peptides administered into the rat ventral tegmental area. *Acta Physiol Scand* **167**, 99–104.

Koch M, Schmid A & Schnitzler HU (2000). Role of muscles accumbens dopamine D1 and D2 receptors in instrumental and Pavlovian paradigms of conditioned reward. *Psychopharmacology (Berl)* **152**, 67–73.

Koyama S & Appel SB (2006). Characterization of M-current in ventral tegmental area dopamine neurons. *J Neurophysiol* **96**, 535–543.

Krashes MJ, Koda S, Ye C, Rogan SC, Adams AC, Cusher DS, Maratos-Flier E, Roth BL & Lowell BB (2011). Rapid, reversible activation of AgRP neurons drives feeding behavior in mice. *J Clin Invest* **121**, 1424–1428.

Labouebe G, Liu S, Dias C, Zou H, Wong JC, Karunakaran S, Clee SM, Phillips AG, Boutrel B & Borgland SL (2013). Insulin induces long-term depression of ventral tegmental area dopamine neurons via endocannabinoids. *Nat Neurosci* **16**, 300–308.

Lacey MG, Mercuri NB & North RA (1987). Dopamine acts on D2 receptors to increase potassium conductance in neurones of the rat substantia nigra zona compacta. *J Physiol* **392**, 397–416.

Lammel S, Hetzel A, Hackel O, Jones I, Liss B & Roeper J (2008). Unique properties of mesoprefrontal neurons within a dual mesocorticolimbic dopamine system. *Neuron* **57**, 760–773.

Lindblom J, Opmane B, Mutulis F, Mutule I, Petrovska R, Klusa V, Bergstrom L & Wikberg JE (2001). The MC4 receptor mediates alpha-MSH induced release of nucleus accumbens dopamine. *Neuroreport* **12**, 2155–2158.

Lippert RN, Ellacott KL & Cone RD (2014). Gender-specific roles for the melanocortin-3 receptor in the regulation of the mesolimbic dopamine system in mice. *Endocrinology* **155**, 1718–1727.

Liu H, Kishi T, Roseberry AG, Cai X, Lee CE, Montez JM, Friedman JM & Elmquist JK (2003). Transgenic mice expressing green fluorescent protein under the control of the melanocortin-4 receptor promoter. *J Neurosci* **23**, 7143–7154.

Liu S & Borgland SL (2015). Regulation of the mesolimbic dopamine circuit by feeding peptides. *Neuroscience* **289**, 19–42.

Lutter M & Nestler EJ (2009). Homeostatic and hedonic signals interact in the regulation of food intake. *J Nutr* **139**, 629–632.

Margolis EB, Toy B, Himmels P, Morales M & Fields HL (2012). Identification of rat ventral tegmental area GABAergic neurons. *PLoS ONE* **7**, e42365.

Mercuri NB, Saiardi A, Bonci A, Picetti R, Calabresi P, Bernardi G & Borrelli E (1997). Loss of autoreceptor function in dopaminergic neurons from dopamine D2 receptor deficient mice. *Neuroscience* **79**, 323–327.

Morales M & Margolis EB (2017). Ventral tegmental area: cellular heterogeneity, connectivity and behaviour. *Nat Rev Neurosci* **18**, 73–85.

Nair-Roberts RG, Chatelain-Badie SD, Benson E, White-Cooper H, Bolam JP & Ungless MA (2008). Stereological estimates of dopaminergic, GABAergic and glutamatergic neurons in the ventral tegmental area, substantia nigra and retrorubral field in the rat. *Neuroscience* **152**, 1024–1031.

Ollmann MM, Wilson BD, Yang YK, Kerns JA, Chen Y, Gantz I & Barsh GS (1997). Antagonism of central melanocortin receptors in vitro and in vivo by agouti-related protein. *Science* **278**, 135–138.

Paladini CA & Roeper J (2014). Generating bursts (and pauses) in the dopamine midbrain neurons. *Neuroscience* **282C**, 109–121.

Palmiter RD (2007). Is dopamine a physiologically relevant mediator of feeding behavior? *Trends Neurosci* **30**, 375–381.

Pandit R, Omrani A, Luijendijk MC, de Vrind VA, Van Rozen AJ, Ophuis RJ, Garner K, Kallo I, Ghanem A, Liposits Z, Conzelmann KK, Vanderschuren LJ, la Fleur SE & Adan RA (2016). Melanocortin 3 receptor signaling in midbrain dopamine neurons increases the motivation for food reward. *Neuropsychopharmacology* **41**, 2241–2251.

Pei H, Patterson CM, Sutton AK, Burnett KH, Myers MG, Jr. & Olson DP (2018). Lateral hypothalamic Mc3R-expressing neurons modulate locomotor activity, energy expenditure and adiposity in male mice. *Endocrinology*.

Pierroz DD, Ziotopoulou M, Ungsunan L, Moschos S, Flier JS & Mantzoros CS (2002). Effects of acute and chronic administration of the melanocortin agonist MTII in mice with diet-induced obesity. *Diabetes* **51**, 1337–1345.

Rice ME, Cragg SJ & Greenfield SA (1997). Characteristics of electrically evoked somatodendritic dopamine release in substantia nigra and ventral tegmental area in vitro. *J Neurophysiol* **77**, 853–862.

Roseberry AG (2013). Altered feeding and body weight following melanocortin administration to the ventral tegmental area in adult rats. *Psychopharmacology (Berl)* **226**, 25–34.

Roseberry AG, Painter T, Mark GP & Williams JT (2007). Decreased vesicular somatodendritic dopamine stores in leptin-deficient mice. *J Neurosci* **27**, 7021–7027.

Roseberry AG, Stuhrman K & Dunigan AI (2015). Regulation of the mesocorticolimbic and mesostriatal dopamine systems by alpha-melanocyte stimulating hormone and agouti-related protein. *Neurosci Biobehav Rev* **56**, 15–25.

Roselli-Rehfuss L, Mountjoy KG, Robbins LS, Mortrud MT, Low MJ, Tatro JB, Entwistle ML, Simerly RB & Cone RD (1993). Identification of a receptor for gamma melanotropin and other proopiomelanocortin peptides in the hypothalamus and limbic system. *Proc Natl Acad Sci U S A* **90**, 8856–8860.

Sanchez MS, Barontini M, Armando I & Celis ME (2001). Correlation of increased grooming behavior and motor activity with alterations in nigrostriatal and mesolimbic catecholamines after alpha-melanotropin and neuropeptide glutamine-isoleucine injection in the rat ventral tegmental area. *Cell Mol Neurobiol* **21**, 523–533.

Shanmugarajah L, Dunigan AI, Frantz KJ & Roseberry AG (2017). Altered sucrose self-administration following injection of melanocortin receptor agonists and antagonists into the ventral tegmental area. *Psychopharmacology (Berl)* **234**, 1683–1692.

Singru PS, Sanchez E, Fekete C & Lechan RM (2007). Importance of melanocortin signaling in refeeding-induced neuronal activation and satiety. *Endocrinology* **148**, 638–646.

Stuhrman K & Roseberry AG (2015). Neurotensin inhibits both dopamine- and GABA-mediated inhibition of ventral tegmental area dopamine neurons. *J Neurophysiol* **114**, 1734–1745.

Swinburn B, Sacks G & Ravussin E (2009). Increased food energy supply is more than sufficient to explain the US epidemic of obesity. *Am J Clin Nutr* **90**, 1453–1456.

Swinburn BA, Sacks G, Hall KD, McPherson K, Finegood DT, Moodie ML & Gortmaker SL (2011). The global obesity pandemic: shaped by global drivers and local environments. *Lancet* **378**, 804–814.

Takahashi KA & Cone RD (2005). Fasting induces a large, leptin-dependent increase in the intrinsic action potential frequency of orexigenic arcuate nucleus neuropeptide Y/agouti-related protein neurons. *Endocrinology* **146**, 1043–1047.

Thompson JL & Borgland SL (2013). Presynaptic leptin action suppresses excitatory synaptic transmission onto ventral tegmental area dopamine neurons. *Biol Psychiatry* **73**, 860–868.

Torre E & Celis ME (1986). Alpha-MSH injected into the substantia nigra or intraventricularly alters behavior and the striatal dopaminergic activity. *Neurochem Int* **9**, 85–89.

Torre E & Celis ME (1988). Cholinergic mediation in the ventral tegmental area of alpha-melanotropin induced excessive grooming: changes of the dopamine activity in the nucleus accumbens and caudate putamen. *Life Sci* **42**, 1651–1657.

Ungless MA, Magill PJ & Bolam JP (2004). Uniform inhibition of dopamine neurons in the ventral tegmental area by aversive stimuli. *Science* **303**, 2040–2042.

Volkow ND, Wang GJ & Baler RD (2011). Reward, dopamine and the control of food intake: implications for obesity. *Trends Cogn Sci* **15**, 37–46.

West KS & Roseberry AG (2017). Neuropeptide-Y alters VTA dopamine neuron activity through both pre- and postsynaptic mechanisms. *J Neurophysiol* **118**, 625–633.

Wise RA (2004). Dopamine, learning and motivation. *Nat Rev Neurosci* **5**, 483–494.

World Health Organization (2018). *Obesity and Overweight*. Available at: http://www.who.int/en/news-room/fact-sheets/detail/obesity-and-overweight [Accessed 28 August 2018].

Wu Q, Lemus MB, Stark R, Bayliss JA, Reichenbach A, Lockie SH & Andrews ZB (2014). The temporal pattern of cfos activation in hypothalamic, cortical, and brainstem nuclei in response to fasting and refeeding in male mice. *Endocrinology* **155**, 840–853.

Yamaguchi T, Sheen W & Morales M (2007). Glutamatergic neurons are present in the rat ventral tegmental area. *Eur J Neurosci* **25**, 106–118.

Yen HH & Roseberry AG (2015). Decreased consumption of rewarding sucrose solutions after injection of melanocortins into the ventral tegmental area of rats. *Psychopharmacology (Berl)* **232**, 285–294.

Zhan C, Zhou J, Feng Q, Zhang JE, Lin S, Bao J, Wu P & Luo M (2013). Acute and long-term suppression of feeding behavior by POMC neurons in the brainstem and hypothalamus, respectively. *J Neurosci* **33**, 3624–3632.

Zhou QY & Palmiter RD (1995). Dopamine-deficient mice are severely hypoactive, adipsic, and aphagic. *Cell* **83**, 1197–1209.

Additional information

Competing interests

The authors declare that they have no competing interests.

Author contributions

The experiments were conducted in the laboratory of Aaron G. Roseberry at Georgia State University. KSW conducted the experiments and drafted the manuscript. DPO generated and provided the MC3R-Cre mice. CL and DPO performed the RNAscope ISH experiments. KSW and AGR analysed and interpreted the results of the experiments. KSW and AGR conceived and designed the work. KSW wrote the initial draft of the manuscript. KSW, AGR and DPO revised the manuscript. All authors approved the final version of the manuscript and agree to be accountable for all aspects of the work in ensuring that questions related to the accuracy or integrity of any part of the work are appropriately investigated and resolved. All persons designated as authors qualify for authorship, and all those who qualify for authorship are listed.

Funding

Funds for these studies were provided by The Brains and Behavior Program at Georgia State University and NIH grant 1R01DK115503 (to AGR).